Biodivers Conserv (2009) 18:2521–2535
DOI 10.1007/s10531-009-9605-7

ORIGINAL PAPER

Mapping potential habitats of threatened plant species in a moist tall grassland using hyperspectral imagery

Jun Ishii · Shan Lu · Syo Funakoshi · Yo Shimizu · Kenji Omasa · Izumi Washitani

Received: 18 October 2007 / Accepted: 19 February 2009 / Published online: 28 February 2009

Abstract We examined the capability of hyperspectral imagery to map habitat types of under-storey plants in a moist tall grassland dominated by *Phragmites australis* and *Miscanthus sacchariflorus*, using hyperspectral remotely-sensed shoot densities of the two grasses. Our procedure (1) grouped the species using multivariate analysis and discriminated habitat types (species groups) based on *P. australis* and *M. sacchariflorus* shoot densities, (2) used estimated shoot densities from hyperspectral data to draw a habitat type map, and (3) analyzed the association of threatened species with habitat types. Our identification of four habitat types, using cluster analysis of the vegetation survey coverage data, was based on *P. australis* and *M. sacchariflorus* shoot density ratios and had an overall accuracy of 77.1% (kappa coefficient = 0.71). Linear regression models based on hyperspectral imagery band data had good accuracy in estimating *P. australis* and *M. sacchariflorus* shoot densities (adjusted $R^2 = 0.686$ and 0.708, respectively). These results enabled us to map under-storey plant habitat types to an approximate prediction accuracy of 0.537. Among the eight threatened species we examined, four exhibited a significantly biased distribution among habitat types, indicating species-specific habitat use. These results suggest that this procedure can provide useful information on the status of potential habitats of threatened species.

Keywords Floodplain wetland · Hyperspectral image · *Miscanthus sacchariflorus* · Multivariate analysis · *Phragmites australis* · Potential habitats · Shoot density · Spatial autocorrelation · Threatened species

Introduction

The recent loss or degradation of wetlands due to human activities is extensive, and wetland conservation and restoration have become of increasing concern worldwide

J. Ishii (✉) · S. Lu · S. Funakoshi · Y. Shimizu · K. Omasa · I. Washitani
Graduate School of Agricultural and Life Sciences, The University of Tokyo,
1-1-1 Yayoi, Bunkyo-ku, Tokyo 113-8657, Japan
e-mail: aishijun@mail.ecc.u-tokyo.ac.jp

(e.g. Whitehead et al. 1990; Sinclair et al. 1995; Edyvane 1999; Gibbs 2000). In Japan, the total wetland area decreased by approximately 40% during the twentieth century, mainly because of urbanization and agricultural development (Ministry of Land, Infrastructure and Transport of Japan 2000). A major type of Japanese lowland wetland, which was once very common even in densely populated areas, is lowland floodplain dominated by the moist tall grasses *Phragmites australis* (Cav.) Trin. ex Steud., *Miscanthus sacchariflorus* (Maxim.) Benth., or both.

A long history of reclamation, especially recent riparian work, has decreased the range of floodplain wetlands and has deprived them of their ecological integrity and associated indigenous plant species (Washitani 2001). Consequently, many of these plants are now listed on the national Red List (Environmental Agency of Japan 2007), making their conservation, as well as that of moist tall grasslands, a priority. However, conservation plan decision-making requires detailed knowledge of both the current distribution of threatened species and dynamic spatio-temporal habitat patterns that govern their long-term persistence and distribution.

A zonation pattern of *P. australis* and *M. sacchariflorus* from deeper water to drier areas is common in Japanese moist tall grasslands. The relative dominances of these species are, therefore, thought to be determined primarily by groundwater level (Yamasaki and Tange 1981; Yamasaki 1990). Both natural and anthropogenic disturbances may also influence these patterns by direct damage to plants or habitat alteration, including changes in hydrological processes, light availability, nutrient status, and other physical environment factors (e.g. Haslam 1972). Such disturbances could be caused by flooding, water level fluctuations, grazing, fire, mowing, ice and wave in wetlands (Keddy 2000). In particular, flooding repeatedly rearranges the environment, destroying certain habitats and creating others (Arscott et al. 2002; Richards et al. 2002). Thus, this habitat complex is a dynamic, shifting mosaic (see Denslow 1985). Spatio-temporal characterization and mapping that reflect the degree of *P. australis* and *M. sacchariflorus* dominance are likely to be pre-requisites to understanding the environmental requirements of under-storey plants, including threatened species.

The use of remote sensing in habitat mapping provides explicit and timely spatial information (reviewed by Mertes 2002; Ozesmi and Bauer 2002), although difficulties in mapping continuous patterns of plant species assemblages still remain (Schmidtlein and Sassin 2004). Recent advances in remote sensors, including hyperspectral sensors, are highly promising for analyzing cover types (including plant species) and their percentages (Turner et al. 2003), in particular dominant species abundance. In a previous study, we demonstrated the technical possibility of using hyperspectral imagery to estimate *P. australis* and *M. sacchariflorus* shoot densities in a moist tall grassland (Lu et al. 2006).

Grouping plant species that share habitats using multivariate analysis may be useful in mapping habitat or vegetation types (Guisan and Zimmermann 2000; Ohmann and Gregory 2002). Dominant species affect the distribution of non-dominant species and hence species groups sharing environmental conditions in a community (e.g. Allen and Forman 1976; Abul-Fatih and Bazzaz 1979; Fowler 1981; Hils and Vankat 1982; Shevtsova et al. 1995; Aksenova and Onipchenko 1998). In a moist tall grassland, the absolute and/or relative abundance of the dominants *P. australis* and *M. sacchariflorus* may be a good predictor of species group habitat types.

In this study, we examined the capability of hyperspectral imagery to map the habitat types of the under-storey plants that constitute the continuous and significant vegetation mosaic of a moist tall grassland, based on remotely-sensed hyperspectral data of *P. australis* and *M. sacchariflorus* shoot densities. In our previous remote sensing study

(Lu et al. 2006), the use of matched filtering, a specialized type of spectral mixture analysis for hyperspectral data, resulted in poor estimates of *P. australis*, due to the difficulty of selecting a pure pixel or endmember. To overcome this technical difficulty, we avoided selecting an endmember by using linear regression models. Shoot densities and band ratios (Ozesmi and Bauer 2002; Galvão et al. 2003) calculated from hyperspectral data were used as the dependent and independent variables, respectively.

Our procedure was composed of the following steps and substeps: (1-1) grouping species sharing similar microhabitat preferences using multivariate analysis and (1-2) identifying the relationship between species group habitat types and *P. australis* and *M. sacchariflorus* shoot densities; (2-1) improving the method to estimate *P. australis* and *M. sacchariflorus* shoot densities from hyperspectral data; (2-2) drawing a habitat type map; and (2-3) analyzing the spatial pattern in the distribution of habitat types; and finally, (3-1) analyzing the association of threatened species with habitat types.

Methods

Study area and analytical strategy

The study was performed in a typical moist tall grassland dominated by *P. australis* and *M. sacchariflorus* located in the eastern part (approximately 16 km^2) of Watarase wetland in central Japan (approximately 33 km^2, 36°11′–36°17′N, 139°40′–139°42′E; Fig. 1). Watarase wetland is a semi-artificially controlled floodplain of three tributaries of the Tone River: the Watarase, Uzuma, and Omoi Rivers. The wetland is valued for controlling floods and its water use in irrigated agriculture, recreational opportunities, and reed harvesting. It also supports rich biodiversity, with more than 650 plant species (Ohwada and Ogura 1996), including 59 species listed on the national Red List (Environmental Agency

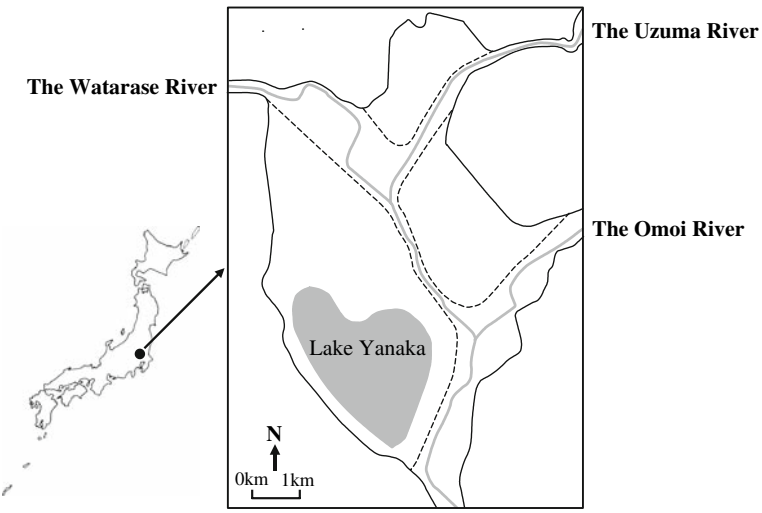

Fig. 1 Location of Watarase wetland in central Japan. Surrounded by urban and agricultural areas, the wetland contains Lake Yanaka and three rivers (*solid gray lines*) that flow into each other. The vegetation is dominated by the moist tall grasses *Phragmites australis* and *Miscanthus sacchariflorus*. *Dotted black lines* represent constructed banks within the wetland

of Japan 2007), including *Amsonia elliptica* (Thunb.) Roem. et Schult., *Apodicarpum ikenoi* Makino, *Arisaema heterophyllum* Blume, *Carex cinerascens* Kükenth., *Euphorbia adenochlora* Morr. et Decne., *Galium tokyoense* Makino, *Ophioglossum namegatae* Nishida et Kurita, and *Thalictrum simplex* var. *brevipes* Hara (Masumi Ohwada, unpublished data).

The annual shoot emergence of *P. australis* and *M. sacchariflorus* usually starts in March, after controlled burns to manage shoot production for commercial use of *P. australis*. The shoots elongate rapidly, reaching maximum height in July–August. Flowering and fruiting occur from September to October and November to December, respectively. The above-ground parts die back in winter, with the rhizomes over-wintering. The average 1976–2005 annual rainfall and air temperature, recorded at Koga Metrological Station near the study area, were approximately 1,187 mm and 14°C.

After observing the spatial variation of *P. australis* and *M. sacchariflorus* shoot densities at several scales in a preliminary field survey, we chose 1–5 m as the measurement and spatial analysis scale.

Figure 2 summarizes our procedure, with individual measurement and analysis steps.

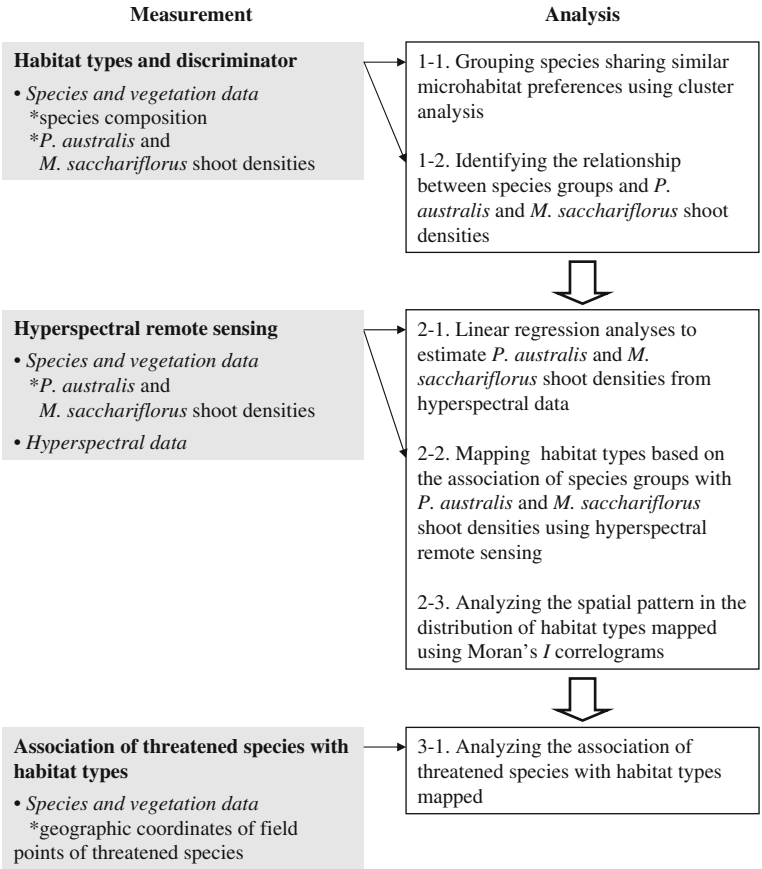

Fig. 2 Study flow chart. Section numbers correspond to study procedure steps

Measurements

Species and vegetation data

A vegetation survey was performed in May–June 2004 and 2005 to obtain data for analyzing the associations between *P. australis* and *M. sacchariflorus* shoot densities and plant species groups (Fig. 2, Sect. 1-1 and 1-2). A total of 613 quadrats (1 × 1 m) were scattered throughout the study area. The locations were selected in a variety of vegetation types in the field and included the maximum ranges of *P. australis* and *M. sacchariflorus* shoot densities. Species composition, coverage (%), and *P. australis* and *M. sacchariflorus* shoot number (=shoot density) were recorded for each quadrat.

Phragmites australis and *M. sacchariflorus* shoot densities for remote-sensing analysis (Fig. 2, Sect. 2-1) were measured from 22 May, the day after an aircraft flew to acquire hyperspectral images, to 14 June 2004. Twenty-three plots (5 × 5 m) were placed within the study area and the locations were selected to include the maximum ranges of *P. australis* and *M. sacchariflorus* shoot densities as possible. In each plot, three quadrats (1 × 1 m) were placed 1 m apart, and data were recorded for each quadrat, with *P. australis* and *M. sacchariflorus* shoot densities calculated as the average over three quadrats. To identify the plot positions on the hyperspectral images, the geographic coordinates of the four corners of each plot were recorded, using a Trimble GPS Pathfinder ProXR (1 m maximum error).

In July 2005, we recorded the geographic coordinates in the southeastern part of the study area of 184 arbitrarily chosen fields points of eight plant species (an average of 43 points per species) that are relatively abundant in the area: *A. elliptica*, *A. ikenoi*, *A. heterophyllum*, *C. cinerascens*, *E. adenochlora*, *G. tokyoense*, *O. namegatae*, and *T. simplex* var. *brevipes* (Fig. 2, Sect. 3-1). The national Red List (Environmental Agency of Japan 2007) designates *A. ikenoi*, *G. tokyoense*, and *O. namegatae* as vulnerable and the others as near vulnerable.

Hyperspectral data

Hyperspectral images were acquired by the airborne imaging spectrometer for applications (AISA) Eagle, which is operated by SPECIM LTD (Spectral Imaging LTD). The instrument collected images at nadir in 68 contiguous bands of reflectance data (bands 1–68), sampled at 8.9 nm intervals in the 398–984 nm spectral wavelength ranges (visible to near infrared). It also has very high radiometric resolution (16 bit). AISA data were collected on 21 May 2004 at 14:37–15:35 local time under clear conditions. The imaging, conducted from an aircraft flying at an altitude of 1,438 m, provided 1.5 m-pixel resolution. Four scenes (each approximately 10 × 1 km) were selected to cover the study area.

The AISA imagery was corrected radiometrically and then atmospherically to apparent on-board reflectance using the Fiber Optic Downwelling Irradiance System (FODIS). The reflectance image value was derived by multiplying the real value by 10,000. Four scenes were mosaicked into one, with estimated positional error <1 pixel, using ERDAS IMAGINE 9.0 (Leica Geosystems Geospatial Imaging, LLC, Norcross, GA). We then transferred the geographic coordinates of the 23 5 × 5 m plots surveyed for *P. australis* and *M. sacchariflorus* shoot densities to the mosaicked scene. The reflectance data of each plot were calculated as the average obtained from all pixels in the plot. Before conducting linear regression analyses to estimate *P. australis* and *M. sacchariflorus* shoot densities

from the hyperspectral data (Fig. 2, Sect. 2-1), all reflectance data were divided by the reflectance value in band 1, to reduce the errors between the images.

Analyses and mapping using hyperspectral imagery

Habitat types and discriminator

To group species sharing similar microhabitats, a hierarchical, agglomerative cluster analysis was performed on the coverage data of the under-storey species recorded in the vegetation survey (613 quadrats) using the Bray–Curtis similarity measure and the flexible linkage method with $\beta = -0.25$ as implemented by PC-ORD for Windows (McCune and Mefford 1999; Fig. 2, Sect. 1-1). *P. australis* and *M. sacchariflorus* were deleted from the data matrix because the association between their shoot densities and species groups identified by the cluster analysis was analyzed in the following step. Species with a frequency of 10% or less were also removed because their presence or absence in a sample may be due to chance alone (McCune and Grace 2002), leaving 25 species for the analysis. Prior to the analysis, the data were transformed by arcsine squareroot transformation to decrease skewness and kurtosis for each species (McCune and Grace 2002). The differences among species groups derived from the cluster analysis were tested by MRPP (multi-response permutation procedure) based on Bray–Curtis similarity.

The four species groups thus recognized were used as habitat types for the following analyses (Fig. 2, Sect. 1-2). The different habitat types were well delineated on the scatter plots by the shoot-density ratios of *P. australis* and *M. sacchariflorus* but not by the shoot density of either species alone, as shown in Fig. 4. Therefore, the shoot density ratio was calculated as a discriminator for each quadrat as: (*M. sacchariflorus* shoot density)/(*P. australis* shoot density + 1). The addition of 1 in the denominator reflects a shoot density of 0 for *P. australis*. The best discriminating value for each habitat type pair was determined as the value that maximized the area under the ROC curve (AUC) values (Hanley and McNeil 1982). The overall performance of the calculated discriminating values was tested by a concordance test with a kappa coefficient (Rosenfield and Fitzpatrick-Lins 1986).

Mapping habitat types based on hyperspectral data

We used linear regression models to estimate *P. australis* or *M. sacchariflorus* shoot densities, based on hyperspectral imagery band data (Fig. 2, Sect. 2-1). To select optimal models, we calculated Akaike's information criterion (AIC; Burnham and Anderson 2002) for all possible candidate models with one or two combinations of variables of 68-band data using *R* (R Development Core Team 2006). The models were ranked based on both delta AIC values (Δ_i) and a measure of the weight of evidence of the best model or Akaike weights (w_i; Burnham and Anderson 2002).

Lu et al. (2007) found that a pre-classification process using the normalized difference vegetation index (NDVI; Thenkabail et al. 2000) to separate the whole image into vegetated and non-vegetated areas improved classification accuracy. We calculated NDVI for the entire study area as: (NIR − red)/(NIR + red), where NIR = 774 nm, red = 675 nm. The vegetation area was extracted when NDVI $\geq$ 0.74 in our AISA scene.

For mapping in these vegetation pixels, *P. australis* and *M. sacchariflorus* shoot densities were estimated using the selected models, and the shoot-density ratio was calculated

(Fig. 2, Sect. 2-2). The habitat type in each pixel was determined by referring to the habitat type discriminator values.

Using the habitat type map obtained in this manner, we analyzed the spatial pattern of habitat types, using Moran's *I* correlograms (Cliff and Ord 1981; Fig. 2, Sect. 2-3), to investigate the effects of our measurement and spatial analysis scale on analyzing and mapping the habitat types. Because habitat types were based on the *P. australis* and *M. sacchariflorus* shoot-density ratio, *I* was calculated for it using *R*. Four investigation areas (100 × 100 m), comprising two nearly pure *P. australis* or *M. sacchariflorus* stands and two areas with large variations in *P. australis* and *M. sacchariflorus* shoot-density ratios, were chosen to include a variety of shoot-density-ratio spatial patterns. We exported the shoot-density ratio data for each area and calculated *I* for five distance classes: 0–3, 3–6, 6–9, 9–12, and 12–15 m. For each distance class, a randomization test with 9,999 permutations (one-tailed test) was performed and the significance of *I* was assessed by a progressive Bonferroni correction (Legendre and Legendre 1998).

Association of threatened species with habitat types

Using geographic coordinates, we layered the locations of the field points of eight threatened species onto the habitat type map we had created and for each species counted the number of points in each habitat type (Fig. 2, Sect. 3-1). To analyze the association of threatened species with habitat type, we performed a goodness of fit test using *R*. For this test, the original chi-squared value was calculated (χ^2_{ori}). All possible contingency tables were generated, and the chi-squared values were calculated (χ^2_{all}). The probability of rejecting the null hypothesis was calculated as: (number of $\chi^2_{all} \geq \chi^2_{ori}$)/(number of χ^2_{all}). The expected value was defined as the number of each habitat type occupied by the 184 data points.

Results

Characterization of habitat types

As noted in the "Methods" section, through cluster analysis of species occurrences within the 613 quadrats, we identified four species groups (Fig. 3). This level of grouping retained

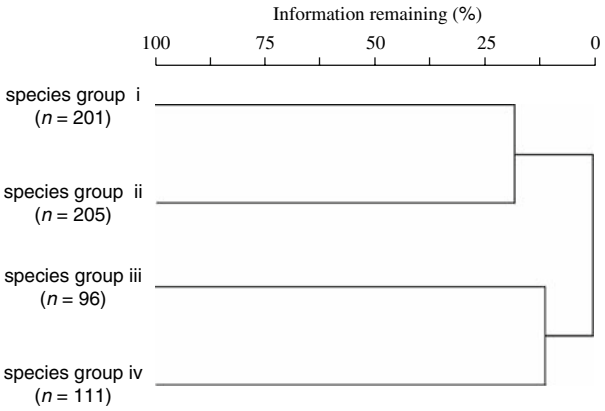

Fig. 3 Dendrogram of the results of hierarchical, agglomerative cluster analysis, grouping 613 quadrats into the four species groups i, ii, iii and iv. The dendrogram is scaled by Wishart's objective function, expressed as the percentage of information remaining at each level of grouping (McCune and Grace 2002). *n* number of quadrats in each group

about 18% of the information in the dendrogram. MRPP showed significant differences among all species groups (chance-corrected within-group agreement $A = 0.342$, $P < 0.001$). Habitat types corresponding to species groups i, ii, iii, and iv were designated as habitat types I, II, III, and IV, respectively.

The best discriminating shoot-density ratio values between habitat types IV and I, I and II, and II and III were 2.5, 0.7, and 0.2, respectively. Based on these values, the four habitat types were discriminated with an overall accuracy of 77.1% (kappa coefficient = 0.71, $P < 0.001$; Table 1). Most omission errors occurred in habitat type II and were associated with the most commission errors in habitat type III (Table 1; Fig. 4).

Habitat types IV, I, II, and III were discriminated as "nearly pure *M. sacchariflorus*", "*M. sacchariflorus*-dominated", "*P. australis*-dominated", and "nearly pure *P. australis*" stands, respectively (Fig. 4).

Mapping habitat types based on hyperspectral data

Model selection results using an information-theoretical approach showed that one model and four models with $\Delta_i < 4$ and with Akaike weights >0.1 could predict *P. australis* and *M. sacchariflorus* shoot densities, respectively (Table 2). The model with the lowest AIC value for *P. australis* was:

$$\text{Shoot density} = 25.487 \times (\text{band58}/\text{band1}) - 9.611 \times (\text{band66}/\text{band1}). \quad (1)$$

The adjusted coefficient of determination (adjusted R^2) was 0.686. The best fitted model for *M. sacchariflorus* density was:

$$\text{Shoot density} = 129.347 \times (\text{band19}/\text{band1}) - 53.078 \times (\text{band36}/\text{band1}) - 234.769. \quad (2)$$

The adjusted R^2 was 0.708. The central wavelengths of band1, 19, 36, 58 and 66 are 397.79, 550.11, 701.42, 901.52 and 974.95 nm, respectively.

Using the shoot-density value estimated by the models to distinguish between the four habitat types, we mapped the ranges of the habitat types (Fig. 5). The overall accuracy of

Table 1 Confusion matrices for accuracy of the discriminating values between the habitat types for species groups identified by cluster analysis (see text and Fig. 3)

Observed habitat types	Accuracy (%)[a]	Number of sites	Estimated habitat types			
			I	II	III	IV
I	75.4	155	117	16	4	18
II	58.7	155	24	91	31	9
III	100	96	0	0	96	0
IV	85.5	110	10	4	2	94
Total		516	151	111	133	121
Reliability accuracy (%)[b]			77.4	82.0	72.2	77.7

The left-hand side (*y* axis) is labeled with the habitat types on the verification sites; the upper edge (*x* axis) is labeled with the same habitat types which refer to those on the verification sites to be evaluated

Overall accuracy (398/516) × 100 = 77.1%

Kappa coefficient = 0.71

[a] (100—percent omission error): also called producer's accuracy

[b] (100—percent commission error): also called user's accuracy

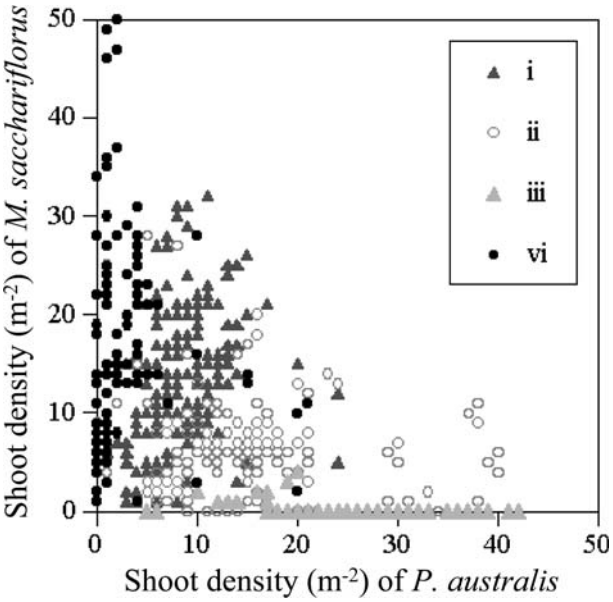

Fig. 4 Scatter plot of *Phragmites australis* and *Miscanthus sacchariflorus* shoot densities in species groups i, ii, iii, and iv (see Fig. 3)

Table 2 Model selection statistics and adjusted R^2 for the analyses of the relationships between both shoot densities of *Phragmites australis* and *Miscanthus sacchariflorus* and hyperspectral reflectance data in Watarase wetland

Model[a]	AIC	Δ_i	w_i	Adjusted R^2
P. australis				
901.52/397.79, 974.95/397.79 nm	167.66	0.00	0.2328	0.686
M. sacchariflorus				
550.11/397.79, 701.42/397.79 nm	181.17	0.00	0.2328	0.708
541.43/397.79, 701.42/397.79 nm	181.98	0.81	0.1556	0.697
532.87/397.79, 576.58/397.79 nm	182.60	1.43	0.1141	0.689
558.93/397.79, 701.42/397.79 nm	182.83	1.66	0.1014	0.686

In hyperspectral reflectance data: band 1, 397.79 nm; band 17, 532.87 nm; band 18, 541.43 nm; band 19, 550.11 nm; band 20, 558.93; band 22, 576.58 nm; band 36, 701.42 nm; band 58, 901.52 nm; band 66, 974.95 nm

[a] Only models with Δ_i smaller than 4 and with Akaike weights greater than 0.1 are shown

the habitat type map was 0.537. This was approximately calculated as: (overall accuracy of discriminating shoot-density-ratio values among habitat types) × (average value of adjusted *P. australis* and *M. sacchariflorus* coefficients of determination) = (77.1/100) × [(0.686 + 0.708)/2]).

Moran's *I* correlograms indicated that *P. australis* and *M. sacchariflorus* shoot-density ratio data, which were exported from the habitat map, showed significant spatial patterns, with *I* decreasing steadily with geographical distance in all four investigation areas (Fig. 6). Overall, *I* was higher in areas of nearly pure *P. australis* or *M. sacchariflorus*

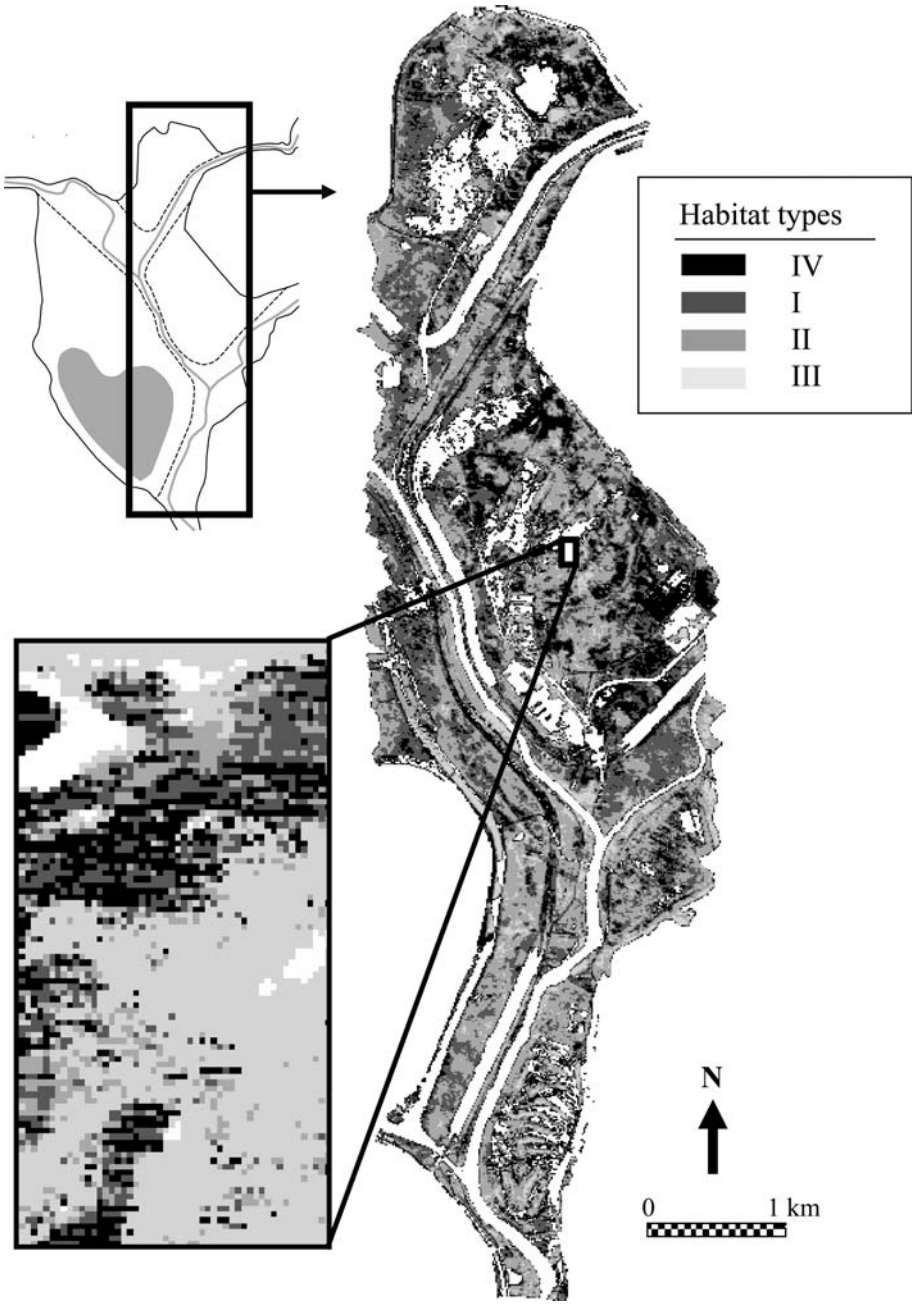

Fig. 5 Habitat type map of moist tall grasslands in Watarase wetland, based on hyperspectral imagery. Pixel size = 1.5 m. Habitat types IV, I, II, and III were identified as "nearly pure *Miscanthus sacchariflorus*", "*M. sacchariflorus*-dominated", "*Phragmites australis*-dominated", and "nearly pure *P. australis*" stands, respectively (see text and Fig. 4)

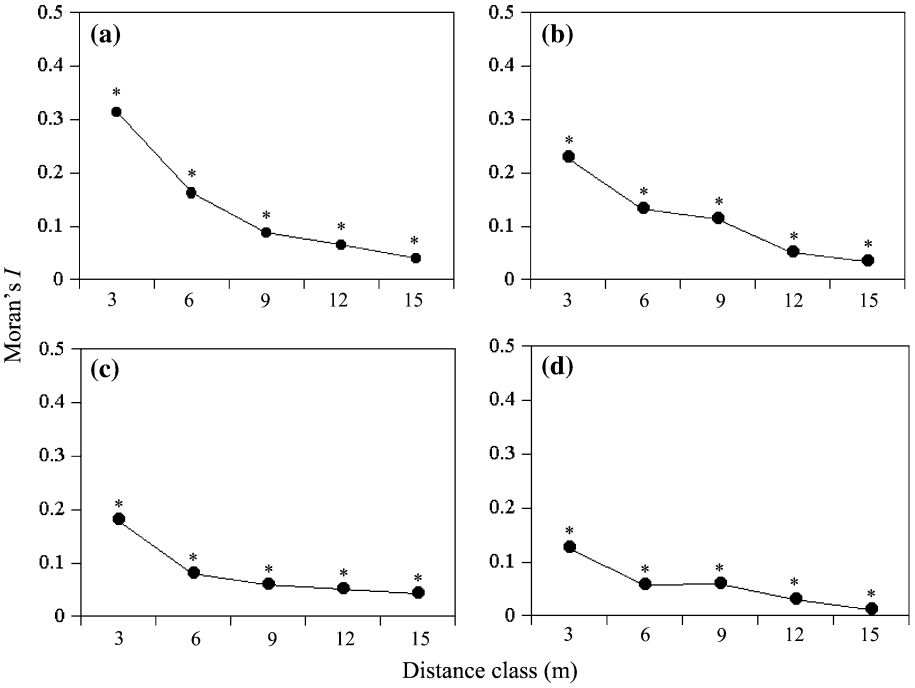

Fig. 6 Moran's *I* correlograms of *Phragmites australis* and *Miscanthus sacchariflorus* shoot-density ratios in four areas: nearly pure *P. australis* stand (**a**), nearly pure *M. sacchariflorus* stand (**b**) and two areas with large shoot-density ratio variations of both species (**c** and **d**). *Asterisks* indicate *I* values that are significant with 5% probability level adjusted using progressive Bonferroni correction

stands than in areas with large variations of *P. australis* and *M. sacchariflorus* shoot-density ratios.

Association of threatened species with habitat types

The threatened species showed fairly typological distribution patterns among the habitat types (Table 3). Four species, *A. elliptica*, *A. ikenoi*, *E. adenochloa*, and *G. tokyoense*, exhibited significantly biased distributions among habitat types. *Amsonia elliptica*, *E. adenochloa*, and *G. tokyoense* were significantly associated with habitat types IV, I, and II, while *A. ikenoi* occurred in habitat type III at significantly higher frequency than expected. No significant associations were detected in four species, *Arisaema heterophyllum*, *Carex cinerascens*, *Ophioglossum namegatae* and *Thalictrum simplex* var. *brevipes*, although each showed a specific trend.

Discussion

Remote sensing of dominant species and habitat mapping

The classification and mapping of a habitat mosaic within a plant community with continuous transitions among plant species assemblages using remotely sensed data is

Table 3 The association of threatened species with four habitat types of a moist tall grassland in Watarase wetland

	n	Habitat types				χ^2	*P*
		IV	I	II	III		
Amsonia elliptica	24	16.7	25.0	50.0	8.3	16.965	**
Apodicarpum ikenoi	83	1.2	9.6	25.3	63.9	9.269	*
Arisaema heterophyllum	40	2.5	5.0	32.5	60.0	5.053	NS
Carex cinerascens	9	0	11.1	11.1	77.8	3.047	NS
Euphorbia adenochlora	54	11.1	24.1	33.3	31.5	8.441	*
Galium tokyoense	44	18.2	20.5	36.4	25.0	14.153	**
Ophioglossum namegatae	72	5.6	16.7	33.3	44.4	1.857	NS
Thalictrum simplex var. *brevipes*	17	0	29.4	41.2	29.4	6.362	NS
All species	184	7.6	14.7	27.7	50.0		

Percentages of the frequencies in which each species was recorded in four habitat types were shown. Habitat types were arranged in order of relative dominance of *Phragmites australis* and *Micanthus sacchariflorus* (see Fig. 4)

* $P < 0.05$; ** $P < 0.01$; *NS* not significant

challenging, due to the low spatial and spectral resolution limitations of remote sensing (Schmidtlein and Sassin 2004). In this study, we sought to map a habitat mosaic of under-storey plants within a moist tall grassland using hyperspectral imagery.

We demonstrated that *P. australis* and *M. sacchariflorus* shoot density ratios were effectual in discriminating habitat types (species groups) with high overall accuracy (77.1%). This enabled us to map the discrete habitat types for the under-storey plants that constituted the continuous vegetation mosaic.

The use of linear regression models resulted in good accuracy in estimating both *P. australis* and *M. sacchariflorus* shoot densities (adjusted coefficients of determination = 0.686 and 0.708, respectively) using hyperspectral imagery and improved the estimator capability of *P. australis* from that in our previous study, which used matched filtering analysis (Lu et al. 2006). Based on these results, we successfully mapped the habitat types of under-storey plants in a moist tall grassland, with an approximate prediction accuracy of 0.537.

Models estimating *P. australis* and *M. sacchariflorus* shoot densities based on hyperspectral data

In the model selections for *P. australis* and *M. sacchariflorus* shoot densities, near-infrared (band 58, 901.52 nm; band 66, 974.95 nm) spectra and both green (band 19, 550.11 nm) and red (band 36, 701.42 nm) spectra were chosen as variables for *P. australis* (Eq. 1) and *M. sacchariflorus* (Eq. 2), respectively. These results are consistent with those of our previous study (Lu et al. 2006), in which spectral differences between *P. australis* and *M. sacchariflorus* occurred in both the 500–560 and of 750–920 nm ranges. Such associations of green, red, and near-infrared spectra with plants are common (e.g. Blackburn 1998; Cochrane 2000; Thenkabail et al. 2000; Kokaly et al. 2003; Schmidt and Skidmore 2003; Mutanga et al. 2004). Our results demonstrate the capability of these spectra to identify plant species.

Spatial patterns of habitat types and their association with threatened species

Significant positive spatial autocorrelations, which recognized lag distances of up to 15 m (equal to the maximum distance in the analyses) for *P. australis* and *M. sacchariflorus* shoot-density ratios in all four investigation areas (two nearly pure *P. australis* and *M. sacchariflorus* stands and two areas with large variations in *P. australis* and *M. sacchariflorus* shoot-density ratios), with relatively high Moran's *I* values within 6 m, suggest that our measurement scale of 1–5 m provided enough spatial resolution to analyze and map the habitat mosaic in the study area. The 6 m^2 maximum quadrat size would work well in assessing the spatial heterogeneity of a moist tall grassland habitat mosaic. Thus, spatial data that retain spatial variations can be acquired through airplane imaging. However, hyperspectral data acquired by satellite sensors, such as Hyperion (30 m resolution), lack sufficient resolution for our vegetation analysis.

The habitat type map with high spatial resolution enabled us to clarify the habitat characteristics of a number of threatened species. Considering that most errors in identifying habitat types were omission errors for habitat type II, leading to habitat type III commission errors, we interpreted the habitat types of the eight threatened species as follows. Whereas both nearly pure *M. sacchariflorus* and *M. sacchariflorus*-dominated stands (habitat types IV and I) were suitable habitat for *A. elliptica*, *E. adenochlora*, and *G. tokyoense*, nearly pure *P. australis* stands (habitat type III) were the favorable type for *A. ikenoi*. These results strongly suggest species-specific habitat use that should be considered in habitat management.

Application of the procedure for mapping potential habitats of threatened species in moist tall grasslands and future research

Our results demonstrated that hyperspectral imagery is capable of mapping the habitat types of the under-storey plants that constitute the continuous vegetation mosaic of moist tall grasslands. Our procedure can be useful for obtaining information on the current status of potential habitats of threatened species and designing strategies to increase survey efficiency and reduce sampling costs of field sampling rare species over larger conservation areas, leading to more cost-effective conservation practices (Guisan et al. 2006; see also Ferrier 2002). It could also be employed to model metapopulation dynamics (Jäkäläniemi et al. 2006; see also Moilanen and Hanski 1998; Löbel et al. 2006). Further investigations are needed to reduce map errors and determine the effectiveness of the same bands of hyperspectral images among different years and sites. With further improvements, our approach may aid in the successful mapping of habitat mosaics in other plant communities as well, and may also contribute to periodical data collection to monitor dynamic spatio-temporal habitat patterns of under-storey species, including threatened species.

Acknowledgments We thank Dr. Miho (Ajima) Nishihiro, Dr. Taku Kadoya, Dr. Shin-ichi Takagawa, Dr. Jun Nishihiro, and Mr. Akira Yoshioka of the University of Tokyo and Mr. Masumi Ohwada for field assistance and advice on data analyses. We also thank two anonymous reviewers for valuable comments on an earlier version of the manuscript.

References

Abul-Fatih HA, Bazzaz FA (1979) The biology of *Ambrosia trifida* L. I. Influence of species removal on the organization of the plant community. New Phytol 83:813–816. doi:10.1111/j.1469-8137.1979.tb02312.x

Aksenova AA, Onipchenko VG (1998) Plant interactions in alpine tundra: 13 years of experimental removal of dominant species. Ecoscience 5:258–270

Allen EB, Forman RTT (1976) Plant species removals and old-field community structure and stability. Ecology 57:1233–1243. doi:10.2307/1935047

Arscott DB, Tockner K, van der Nat D, Ward JV (2002) Aquatic habitat dynamics along a braided alpine river ecosystem (Tagliamento River, Northeast Italy). Ecosystems (N Y, Print) 5:802–814

Blackburn GA (1998) Quantifying chlorophylls and carotenoids at leaf and canopy scales: an evaluation of some hyperspectral approaches. Remote Sens Environ 66:273–285. doi:10.1016/S0034-4257(98)00059-5

Burnham KP, Anderson DR (2002) Model selection and multimodel inference: a practical information-theoretic approach, 2nd edn. Springer, New York

Cliff AD, Ord JK (1981) Spatial processes: models and applications. Pion, London

Cochrane MA (2000) Using vegetation reflectance variability for species level classification of hyperspectral data. Int J Remote Sens 21:2075–2087. doi:10.1080/01431160050021303

Denslow JS (1985) Disturbance-mediated coexistence of species. Academic Press, New York

Edyvane KS (1999) Coastal and marine wetlands in Gulf St. Vincent, South Australia: understanding their loss and degradation. Wetlands Ecol Manage 7:83–104. doi:10.1023/A:1008481228129

Environmental Agency of Japan (2007) Red List of threatened plants of Japan. http://www.env.go.jp/press/file_view.php?serial=9947&hou_id=8648 (in Japanese). Cited 25 Jan 2009

Ferrier S (2002) Mapping spatial pattern in biodiversity for regional conservation planning: where to from here? Syst Biol 51:331–363. doi:10.1080/10635150252899806

Fowler N (1981) Competition and coexistence in a North Carolina grassland II. The effects of the experimental removal of species. J Ecol 69:843–854. doi:10.2307/2259640

Galvão LS, Filho WP, Abdon MM, Novo EMML, Silva JSV, Ponzoni FJ (2003) Spectral reflectance characterization of shallow lakes from the Brazilian Pantanal wetlands with field and airborne hyperspectral data. Int J Remote Sens 24:4093–4112. doi:10.1080/0143116031000070382

Gibbs JP (2000) Wetland loss and biodiversity conservation. Conserv Biol 14:314–317. doi:10.1046/j.1523-1739.2000.98608.x

Guisan A, Zimmermann NE (2000) Predictive habitat distribution models in ecology. Ecol Modell 135:147–186. doi:10.1016/S0304-3800(00)00354-9

Guisan A, Broennimann O, Engler R, Vust M, Yoccoz NG, Lehmann A, Zimmermann NE (2006) Using niche-based models to improve the sampling of rare species. Conserv Biol 20:501–511. doi:10.1111/j.1523-1739.2006.00354.x

Hanley JA, McNeil BJ (1982) The meaning and use of the area under a receiver operating characteristic (ROC) curve. Radiology 143:29–36

Haslam SM (1972) *Phragmites communis* Trin. J Ecol 60:585–610. doi:10.2307/2258363

Hils MH, Vankat JL (1982) Species removals from a first-year old-field plant community. Ecology 63:705–711. doi:10.2307/1936791

Jäkäläniemi A, Tuomi J, Siikamäki P (2006) Conservation of species in dynamic landscapes: divergent fates of *Silene tatarica* populations in riparian habitats. Conserv Biol 20:844–852. doi:10.1111/j.1523-1739.2006.00348.x

Keddy PA (2000) Wetland ecology: principles and conservation. Cambridge University Press, Cambridge

Kokaly RF, Despain DG, Clark RN, Livo KE (2003) Mapping vegetation in Yellowstone National Park using spectral feature analysis of AVIRIS data. Remote Sens Environ 84:437–456. doi:10.1016/S0034-4257(02)00133-5

Legendre P, Legendre L (1998) Numerical ecology, 2nd edn. Elsevier Science, Amsterdam

Löbel S, Snäll T, Rydin H (2006) Metapopulation processes in epiphytes inferred from patterns of regional distribution and local abundance in fragmented forest landscapes. J Ecol 94:856–868. doi:10.1111/j.1365-2745.2006.01114.x

Lu S, Funakoshi S, Shimizu Y, Ishii J, de Asis AM, Ajima M, Washitani I, Omasa K (2006) Estimation of plant abundance and distribution of *Miscanthus sacchariflorus* and *Phragmites australis* using matched filtering of hyperspectral image. Eco-Engineering 18:65–70

Lu S, Oki K, Shimizu Y, Omasa K (2007) Comparison between several feature extraction/classification methods for mapping complicated agricultural land use patches using airborne hyperspectral data. Int J Remote Sens 28:963–984. doi:10.1080/01431160600771561

McCune B, Grace JB (2002) Analysis of ecological communities. MjM Software, Gleneden Beach

McCune B, Mefford MJ (1999) Multivariate analysis of ecological data, Vers 4.20. MjM Software, Gleneden Beach

Mertes LAK (2002) Remote sensing of riverine landscapes. Freshw Biol 47:799–816. doi:10.1046/j.1365-2427.2002.00909.x

Ministry of Land, Infrastructure and Transport of Japan (2000) Lake and Wetland Survey of Geographical Survey Institute (in Japanese). http://www1.gsi.go.jp/geoww/lake/index.html
Moilanen A, Hanski I (1998) Metapopulation dynamics: effects of habitat quality and landscape structure. Ecology 79:2503–2515
Mutanga O, Skidmore AK, Prins HHT (2004) Predicting in situ pasture quality in the Kruger National Park, South Africa, using continuum-removed absorption features. Remote Sens Environ 89:393–408. doi:10.1016/j.rse.2003.11.001
Ohmann JL, Gregory MJ (2002) Predictive mapping of forest composition and structure with direct gradient analysis and nearest-neighbor imputation in coastal Oregon USA. Can J For Res 32:725–741. doi:10.1139/x02-011
Ohwada M, Ogura H (1996) A floristic study of the Watarase retarding basin. Bull Tochigi Pref Mus 13: 31–108 In Japanese with English abstract
Ozesmi SL, Bauer ME (2002) Satellite remote sensing of wetlands. Wetlands Ecol Manage 10:381–402. doi:10.1023/A:1020908432489
R Development Core Team (2006) R: a language and environment for statistical computing. R Foundation for Statistical Computing, Vienna
Richards K, Brasington J, Hughes F (2002) Geomorphic dynamics of floodplains: ecological implications and a potential modelling strategy. Freshw Biol 47:559–579. doi:10.1046/j.1365-2427.2002.00920.x
Rosenfield GH, Fitzpatrick-Lins K (1986) A coefficient of agreement as a measure of thematic classification accuracy. Photogramm Eng Rem S 52:223–227
Schmidt KS, Skidmore AK (2003) Spectral discrimination of vegetation types in a coastal wetland. Remote Sens Environ 85:92–108. doi:10.1016/S0034-4257(02)00196-7
Schmidtlein S, Sassin J (2004) Mapping of continuous floristic gradients in grasslands using hypersperctral imagery. Remote Sens Environ 92:126–138. doi:10.1016/j.rse.2004.05.004
Shevtsova A, Ojala A, Neuvonen S, Vieno M, Haukioja E (1995) Growth and reproduction of dwarf shrubs in a subarctic plant community: annual variation and above-ground interactions with neighbours. J Ecol 83:263–275. doi:10.2307/2261565
Sinclair ARE, Hik DS, Schmitz OJ, Scudder GGE (1995) Biodiversity and the need for habitat renewal. Ecol Appl 5:579–687. doi:10.2307/1941968
Thenkabail PS, Smith RB, Pauw ED (2000) Hyperspectral vegetation indices and their relationships with agricultural crop characteristics. Remote Sens Environ 71:158–182. doi:10.1016/S0034-4257(99)00067-X
Turner W, Spector S, Gardiner N, Fladeland M, Sterling E, Steininger M (2003) Remote sensing for biodiversity science and conservation. Trends Ecol Evol 18:306–314. doi:10.1016/S0169-5347(03)00070-3
Washitani I (2001) Plant conservation ecology for management and restoration of riparian habitats of lowland Japan. Popul Ecol 43:189–195. doi:10.1007/s10144-001-8182-8
Whitehead PJ, Wilson BA, Bowman DMJS (1990) Conservation of coastal wetlands of the Northern Territory of Australia: the Mary River floodplain. Biol Conserv 52:85–111. doi:10.1016/0006-3207(90)90119-A
Yamasaki S (1990) Population dynamics in overlapping zones of *Phragmites australis* and *Miscanthus sacchariflorus*. Aquat Bot 36:367–377. doi:10.1016/0304-3770(90)90053-N
Yamasaki S, Tange I (1981) Growth responses of *Zizania latifolia*, *Phragmites australis* and *Miscanthus sacchariflorus* to varying inundation. Aquat Bot 10:229–239. doi:10.1016/0304-3770(81)90025-5